Cellulose (2018) 25:1743–1756
https://doi.org/10.1007/s10570-018-1671-0

ORIGINAL PAPER

Utilization of pineapple peel for production of nanocellulose and film application

Hongjie Dai · Shiyi Ou · Yue Huang · Huihua Huang

Received: 28 June 2017 / Accepted: 22 January 2018 / Published online: 3 February 2018

Abstract Pineapple peel is a renewable agricultural residue available in abundance whose multipurpose utilization deserves more attention. The present study aimed at the isolation of nanocellulose from pineapple peel and evaluation on its reinforcement capability for gellan gum film. The results from scanning electron microscopy (SEM), Fourier transform infrared spectroscopy (FTIR) and X-ray diffraction (XRD) indicated the progressive removal of non-cellulosic components and the non-destruction of cellulose structure following bleaching and alkali treatments. Atomic force microscopy image of the nanocellulose displayed a needle-like structure with averages of 15 ± 5 nm in diameter and 189 ± 23 nm in length. Thermal gravimetric analysis (TGA) indicated that the obtained fibres after bleaching and alkali treatments showed higher thermal stability than the untreated pineapple peel. Although showing an earlier initial degradation temperature, the obtained nanocellulose remained the maximum residue after being heated to 500 °C. The rheological results indicated that the viscosities of the nanocellulose/gellan gum solutions increased slightly with the increase of nanocellulose content. The prepared films were characterized by FTIR, SEM, XRD, TGA, light transmittance and mechanical properties. The introduction of nanocellulose decreased light transmittance values but enhanced the thermal stability of gellan gum film. Compared with the neat gellan gum film, the 4% nanocellulose loaded gellan gum film showed 48.21% improvement in tensile strength.

Keywords Pineapple peel · Nanocellulose · Characterization · Gellan gum · Film

H. Dai · Y. Huang · H. Huang (✉)
School of Food Science and Engineering, South China University of Technology, No. 381, Wushan Road, Tianhe District, Guangzhou City 510641, Guangdong Province, China
e-mail: fehhuang@scut.edu.cn

S. Ou
Department of Food Science and Engineering, Jinan University, Guangzhou 510632, China

Introduction

In recent years, many works have been devoted to producing sustainable and environmental friendly materials due to the increasing concerns on severe environmental pollution. So, the utilization of biomass residues as feedstock for application in energy and materials becomes the object of intensive academic and industrial research (Santos et al. 2013). Cellulose is an extensive crystalline homo-polymer of anhydroglucopyranose units (AGU) via β-1,4-glycosidic linkage and intra- and inter-molecular hydrogen bonds (Dai and Huang 2017a, b; Nepomuceno et al. 2017; Saelo et al. 2016). As one of the most abundant natural polymers on the earth (a yearly production of about

1.5×10^{12} tons), cellulose has received increasing research interest owing to its environmental friendly advantages and attractive features, such as nontoxicity, biological biodegradation, biocompatibility, excellent thermal and mechanical properties, renewability and easy modification (Dai and Huang 2016, 2017a, b; Khawas and Deka 2016; Zhang et al. 2017a, b).

Recently, highly crystalline nanoscale materials, namely cellulose nanocrystals (CNCs) or reported in the literature as whiskers, nanofibers, nanocelluloses, cellulose crystallites or crystals, have garnered more and more interest due to attractive characteristics, including biocompatibility, biodegradability, light weight, non-toxicity, stiffness, renewability, sustainability, optical transparency, low thermal expansion, gas impermeability, adaptable surface chemistry, and improved mechanical properties (Lagerwall et al. 2014; Trache et al. 2017). Hence CNCs potentially have application in nanocomposites, papers, coating additives, electrolytes, foams, aerogels, food packaging, and gas barriers (Abdul Khalil et al. 2014; Brinchi et al. 2013; Hu et al. 2013a, b; Sharmin et al. 2012). Generally, CNCs are needle-shaped nanometric or rod-like particles with at least one dimension equal to or less than 100 nm (Flauzino Neto et al. 2013). CNCs are traditionally obtained by acid hydrolysis through partially dissolving cellulose fibrils (Feng et al. 2015; Nepomuceno et al. 2017). Naturally, cellulose molecular chains are biosynthesized, self-assembled and repeatedly aggregated along cellulose chains to form microfibrils, composed of crystalline and amorphous domains (Haafiz et al. 2014). The amorphous regions in cellulose structure are preferentially hydrolyzed and removed when being subjected to strong acid hydrolysis, while the crystalline regions are not easily hydrolyzed due to their higher resistance to acid (Feng et al. 2015). The most common hydrolyzing agent is sulfuric acid, which can react with the surface hydroxyl groups of cellulose via an esterification process by allowing the grafting of anionic sulfate ester groups. The production of these negatively charged groups can promote dispersion of the nanocellulose in water by electrostatic repulsion (Dufresne 2013; Feng et al. 2015). In the last decade, agricultural wastes or by-products such as rice husk (Johar et al. 2012), pineapple leaf (Santos et al. 2013), pine wood and corncob (Ditzel et al. 2017), soy hulls (Flauzino Neto et al. 2013), kelp residue (Feng et al. 2015), banana peel (Khawas and Deka 2016), oil palm biomass (Haafiz et al. 2014), sugarcane bagasse (Mandal and Chakrabarty 2011), red algae marine biomass (Chen et al. 2016), and sugar beet pulp (Li et al. 2014) have been investigated as the sources for producing CNCs.

Pineapple, as one of the most popular typical tropic fruits, is produced in the world totaling 16–19 million tonnes annually (Dai and Huang 2016). Pineapple is primarily consumed as fresh fruit and juice, and also available as food complements in desserts, salads, fruit cocktail, jam, juice combinations or can food processing industries, and can be a source of bromelain (Dai and Huang 2017a, b; Kaur et al. 2016; Krishni and Hameed 2014). However, pineapple peel, accounting for 35% of the total pineapple weight, is generated during the pineapple processing. Here it is worth noting that the disposal of pineapple peel is costly and its deposition on a large scale can cause serious environmental issues (Hu et al. 2010). Hence from a waste processing point of view, pineapple peel should be a good biomass obtained without any additional cost input for industrial purposes. Pineapple peel is principally composed of cellulose, hemicellulose, lignin and pectin in which cellulose generally accounts for 20–25% of the dry weight of pineapple peel according to our previous works (Dai and Huang 2016, 2017a, b). Hence, the multipurpose utilization of pineapple peel is of important significance, especially in the use of cellulose. Until now, there have been some reports on the utilization of pineapple peel, including cellulose extraction (Zhang and Xia 2012), bromelain extraction (Kaur et al. 2016), activated carbons (Foo and Hameed 2012), methanolic and biogas productions (Choonut et al. 2014), and adsorbents (Bhatnagar and Sillanp 2010). Recently, our laboratory also reported on the use of pineapple peel as the material for isolating cellulose and preparing cellulose-based hydrogels (Dai and Huang 2016, 2017a, b; Dai et al. 2017, 2018a, b; Hu et al. 2010, 2013a, b).

Gellan gum (GGm) is a linear anionic extracellular polysaccharide isolated from bacterium *Sphingomonas elodea* (originally named *Pseudomonas elodea*) with a repeated tetrasaccharide unit of β-D-glucose, β-D-glucuronic acid, and α-L-rhamnose units at a molar ratio of 2:1:1 (Xu et al. 2007). Due to low toxicity, biodegradability, stability to acid and alkali as well as gelatinity, GGm is intensively applied in the food industry as a food additive approved by the FDA (Karim and Bhat 2008). More recently, regarding the

excellent film-forming ability, a series of films based on GGm have been investigated for applications in drug delivery (Xu et al. 2007), anti-adhesion barrier (Lee et al. 2012), bone regeneration (Chang et al. 2010), transparent dressing materials (Ismail et al. 2014), antioxidant materials (Criado et al. 2015) and paper cups (Zhang et al. 2017a, b).

The main objectives of the present study are to isolate nanocellulose from pineapple peel and then evaluate its potential application in GGm films. To achieve these objectives, nanocellulose was firstly obtained using sulfuric acid hydrolysis preceded by bleaching and alkali treatment. The characterization and comparison were conducted by Fourier transform infrared spectroscopy (FTIR), scanning electron microscopy (SEM), X-ray diffraction (XRD), thermogravimetry (TG), and atomic force microscopy (AFM). The films were then prepared by casting and water evaporation, and characterized by FTIR, SEM, XRD and TG. Moreover, the effects of nanocellulose on the light transmittance and mechanical properties of the films were investigated.

Materials and methods

Materials and reagents

Pineapple peel at mature edible stage was obtained from a local pineapple processing factory (Guangzhou City, China). Gellan gum (GelzanTM, low-acyl form) was provided by Sigma-Aldrich (USA). Sodium chlorite ($NaClO_2$), used for bleach treatment, was purchased from Shanghai Aladdin Reagent Co., Ltd. (Shanghai, China). Sodium hydroxide (NaOH), used for alkali treatment, was supplied by Tianjin Fuchen Chemical Reagent Co., Ltd. (Tianjin City, China). All other chemicals used in this experiment were of analytical grade and solutions were prepared with distilled water.

Preparation of pineapple peel cellulose

Cellulose was isolated from the pineapple peel according to the method described by Hu et al. (2010) with some modifications. The collected pineapple peel was cleaned thoroughly with running tap water followed by soaking in distilled water for 1.0 h to remove dirt or dust. After being dried and pulverized, the powdered pineapple peel (untreated PP) was firstly stir-treated with distilled water at a liquor ratio of 1:20 g/mL and 80 °C for 2 h. The residue was subsequently delignified with 7.5% (w/v) sodium chlorite solution (pH 3.8-4.0, adjusted by 4 mol/L hydrochloric acid solution) at 75 °C for 2 h. After filtration, the residue was washed with distilled water until the washing liquid turned colourless. Then the residue (bleach-treated PP) was stir-treated with 10% (w/v) sodium hydroxide solution at room temperature for 10 h to remove hemicellulose, followed by washing with distilled water and 95% ethanol by turns until the filtrate turned neutral. The residue was then dried in an oven at 50 °C until a constant weight was reached. Finally, the pineapple peel cellulose (PPC) was available after pulverizing into particle size from 150 to 200 μm.

Isolation of pineapple peel nanocellulose

Isolation of pineapple peel nanocellulose was performed using acid hydrolysis method described in the reports (Mandal and Chakrabarty 2011; Santos et al. 2013). Briefly, the obtained PPC (about 10 g) was hydrolyzed in 64% (w/w) sulfuric acid at a liquor ratio of 1:20 g/mL and 50 °C for 45 min under vigorous and constant stirring. Subsequently, the hydrolysis was diluted by adding tenfold cold distilled water and then centrifugated at 5000 rpm for 10 min. After discarding the supernatant, the precipitate was collected and continuously washed with cold distilled water and then centrifuged again. The washing-centrifuging process was repeated until the supernatant turned turbid (about 4 washing–centrifuging cycles). The collected suspension was dialyzed against distilled water for 72 h at 4 °C. Finally, the resulting suspension was sonicated for 30 min and stored at 4 °C for further use (for the films preparation). The dried pineapple peel nanocellulose (noted as PPNc) was obtained using a vacuum freeze drier at − 50 °C for 24 h. The yield of PPNc isolated from PPC by the above processing was almost 21%. The brief preparation procedure for PPNc is depicted in Scheme 1.

Preparation of GGm/PPNc films

The GGm/PPNc films were prepared by casting and evaporation process also as depicted in Scheme 1. Briefly, 1% (w/w) of GGm solution containing varied amount of PPNc (2, 4, 6, 8 and 10% of gellan gum,

Scheme 1 Experimental procedure for PPNc preparation and its application in GGm films

w/w) was prepared using distilled water as a solvent, followed by addition of glycerol (15% of gellan gum, w/w) as a plasticizer. After complete dissolution and dispersion, the mixed solutions were sonicated for 10 min and subsequently cast on a clean glass plate. The obtained film (noted as GGm/PPNc(x)-F, x represents the amount of PPNc) was peeled off from the plate after the water fully evaporated at room temperature. The neat GGm film (noted as GGm-F) was also prepared by the above process except the addition of PPNc.

Characterization

Fourier transform-infrared spectroscopy

FTIR spectra of the samples were recorded using a FTIR spectrometer (Vector 33, Bruker, Germany) in transmittance mode at a resolution of 4 cm^{-1} from 400 to 4000 cm^{-1}. Prior to analysis, the samples were grounded with potassium bromide (KBr) (1:100, w/w) and pressed into transparent pellets.

X-ray diffraction

XRD patterns of the samples were obtained using an X-ray diffractometer (D8 ADVANCE, Bruker, Germany) with Cu-Ka radiation ($\lambda = 0.15418$ nm) at a voltage of 40 kV and a current of 40 mA. XRD data were collected within a 2θ range of 4°–50° at a scanning speed of 2°/min. In order to evaluate the crystallinity of the obtained fibres, the crystallinity index (CrI) was calculated by the following Segal equation (Nam et al. 2016):

$$CrI(\%) = \frac{I_{200} - I_{am}}{I_{200}} \times 100$$

where I_{200} is the maximum intensity of the (200) diffraction peak for cellulose Iβ at $2\theta = 22.5°$ and I_{am} is the intensity of diffraction for amorphous part at $2\theta = 18.5°$.

Scanning electron microscopy

SEM images of the samples were observed using a field emission scanning electron microscope (S-

3700N, Hitachi, Japan) at an acceleration voltage of 15 kV. Prior to analysis, the samples were gold-coated for 60 s using a sputter coater (Cressington 108 auto, Watford, UK). For each sample, at least five SEM images were captured from random areas.

Atomic force microscopy

The AFM force mapping of PPNc was performed in air on triplicate samples in order to avoid the damage of the surface analyzed, using an atomic force microscope (Multimode 8, Bruker, Germany). Height and phase images were obtained simultaneously in tapping mode at the resolution of 256 × 256 point. Prior to analysis, a drop of a diluted PPNc suspension (0.01%, w/w) was deposited onto a freshly cleaved mica surface and dried at room temperature for 4 h.

Thermal analysis

Thermal characterization of the samples was performed by thermal gravimetric analysis (TGA) using a thermal analyzer (STA449C, NETZSCH, Germany) from room temperature to 500 °C at a constant heating rate of 10 °C/min under N_2 atmosphere.

Zeta potential measurements

The zeta potential of PPNc suspension was measured at 25 °C using a zeta potential analyzer (SZ-100 Nanoparticle, Horiba, Germany). Prior to analysis, the suspension was diluted to a concentration of 0.01% (w/w) with distilled water and ultrasonicated for 30 min.

Rheological studies of GGm/PPNc aqueous solutions

The rheological measurements of the aqueous solutions containing 1% of gellan gum and varied amount of PPNc (respectively 0, 2, 4, 6, 8 and 10% of gellan gum, w/w) were performed using a rheometer (RS600, Haake Co., Germany), equipped with a Universal Peltier system and water bath (MultiTemp III, Amersham Biosciences) for temperature control. A parallel plate of 27.83 mm in diameter was used, and the gap was set at 1.0 mm. The flow measurements were performed at an increasing shear rate from 0.1 to 100 s^{-1}. All measurements were conducted within the linear viscoelastic region and rheological measurements were carried out at a reference temperature 25 °C.

Light transmittance testing of the films

The light transmittance (Tr) of the prepared films was measured using an UV–Vis spectrophotometer (UV 1800, Shimadzu, Japan) at a wavelength range of 200–900 nm.

Mechanical properties of the films

Mechanical properties of the prepared films were analyzed using a Texture Analyser TA-XT-plus (Stable Micro Systems, Surrey, UK) according to ASTM standard method D882, with a 50 N load cell equipped with tensile grips (A/TG model). Prior to analysis, the films were cut into neat small blocks with 10 mm wide and 80 mm long strips. The initial grip separation and cross-head speed were set at 50 mm and 60 mm/min, respectively. The values of tensile strength (TS) and elongation at break (EC) were evaluated and reported as the average values of five measurements of each film.

Results and discussion

FTIR spectra analysis

The FTIR spectra of the untreated PP, bleach-treated PP, PPC and PPNc are shown in Fig. 1a. All these samples showed a broad and strong peak at 3450–3400 cm^{-1} and a relative weak peak at 2900 cm^{-1} due to the stretching vibrations of O–H and C–H groups in cellulose molecules respectively (Mandal and Chakrabarty 2011). The peak at 1736 cm^{-1} observed in the untreated PP is ascribed to the acetyl and ester groups in hemicellulose component or the ester linkage between the carboxylic group of ferulic and p-coumaric acids of lignin and/or hemicelluloses (Santos et al. 2013). Compared with the untreated PP, the peak at 1736 cm^{-1} was found decreased in the bleach-treated PP due to the removal of lignin and totally disappeared in PPC due to the completed removal of hemicellulose and lignin. Additionally, the weak peak at 1517 cm^{-1} in the untreated PP is considered as the characteristic of lignin and attributed for C=C vibration (Flauzino Neto et al. 2013), which also completely disappeared in the bleach-treated PP, PPC and PPNc, further indicating the successful removal of lignin. The peak at 1650 cm^{-1} in all samples involves the O–H bending of the absorbed

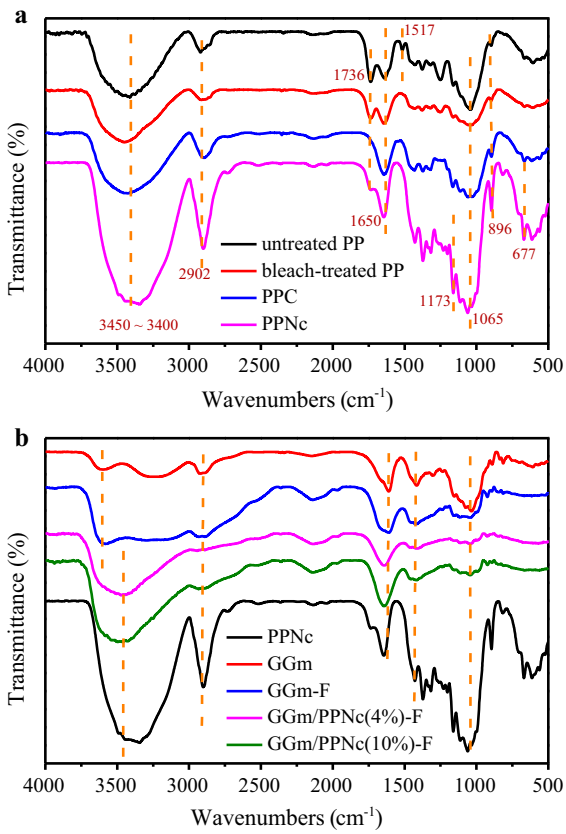

Fig. 1 FTIR spectra of untreated PP, bleach-treated PP, PPC and PPNc (**a**), GGm, GGm-F, GGm/PPNc(4%)-F and GGm/PPNc(10%)-F (**b**)

water molecules due to a strong interaction between cellulose and water (Haafiz et al. 2014). The peak at 1065 cm^{-1} is ascribed to the C–O–C pyranose ring (antisymmetric in phase ring) stretching vibration, and the peak at 896 cm^{-1} is associated with the C-H rocking vibration of typical cellulose (anomeric vibration, specific for β-glucosides) (Haafiz et al. 2014). Generally, the increase of these two peaks involves the increase of cellulosic components (Santos et al. 2013). After bleaching, alkali and acid hydrolysis treatments, the obtained PPNc showed higher peak intensity at 1065 and 896 cm^{-1}, implying the higher relative content of cellulose. FT-IR spectra of PPNc were similar to that of PPC in all wavenumbers, suggesting the non-destruction of the main cellulose structures. However, two new peaks at 1173 and 677 cm^{-1} were observed for PPNc, corresponding to the presence of SO_4^{2-} groups (Feng et al. 2015; Morais et al. 2013). These results indicate the effectiveness of a multiple-step treatment for the successful removal of non-cellulosic components and the non-destruction of cellulose structures.

The FTIR spectra of the prepared films (GGm-F, GGm/PPNc(4%)-F, GGm/PPNc(10%)-F) and their initial compositions (GGm and PPNc) are shown in Fig. 1b. In the case of GGm-F, the broad peak at 3400–3000 cm^{-1} is associated with the O–H stretching vibration and the peak at 2901 cm^{-1} was ascribed to the C–H stretching vibration (Kulkarni et al. 2011). The peaks observed at 1600 and 1411 cm^{-1} are due to the presence of asymmetric carboxylate anion stretching and symmetric carboxylate anion stretching, respectively (Yang et al. 2013). The peak at 1033 cm^{-1} is attributed to C–O–C stretching vibration (Haafiz et al. 2014). For GGm/PPNc(4%)-F and GGm/PPNc(10%)-F, there were no new peaks different from those of the components, indicating no chemical reaction occurred between GGm and PPNc during the film preparation process. Compared with the neat GGm film (GGm-F), the composite films GGm/PPNc(4%)-F and GGm/PPNc(10%)-F showed an increased intensity of peak for O–H groups, implying an increased hydrogen bonds interactions between GGm and PPNc.

XRD patterns analysis

The XRD patterns of the untreated PP, bleach-treated PP, PPC and PPNc are shown in Fig. 2a. All samples exhibited crystalline peaks at $2\theta = 16.1°$, 22.5° and 34.6°, corresponding to the (1−10)/(110) overlapping, (200), and (004) planes of the typical structure of cellulose Iβ, respectively (French 2014; Feng et al. 2015). These observations also suggested that the crystalline structure of cellulose Iβ was maintained after bleaching, alkali and acid hydrolysis treatments. Interestingly, two new peaks were observed at $2\theta = 12.1°$ and 20.1° for PPNc, suggesting the allomorph coexistence of cellulose I and cellulose II (Shankar and Rhim 2016). The possible explanation might be related with the re-precipitation of the cellulose after acid hydrolysis treatment, during which the 64% sulfuric acid solution might be a solvent for cellulose (Flauzino Neto et al. 2013). A similar phenomenon was also observed for cellulose nanocrystals from soy hulls residues (Flauzino Neto et al. 2013), sugarcane bagasse (Mandal and Chakrabarty 2011), and oil palm biomass (Haafiz et al. 2014).

The calculated crystallinity index (CrI) values for the untreated PP, bleach-treated PP, PPC and PPNc

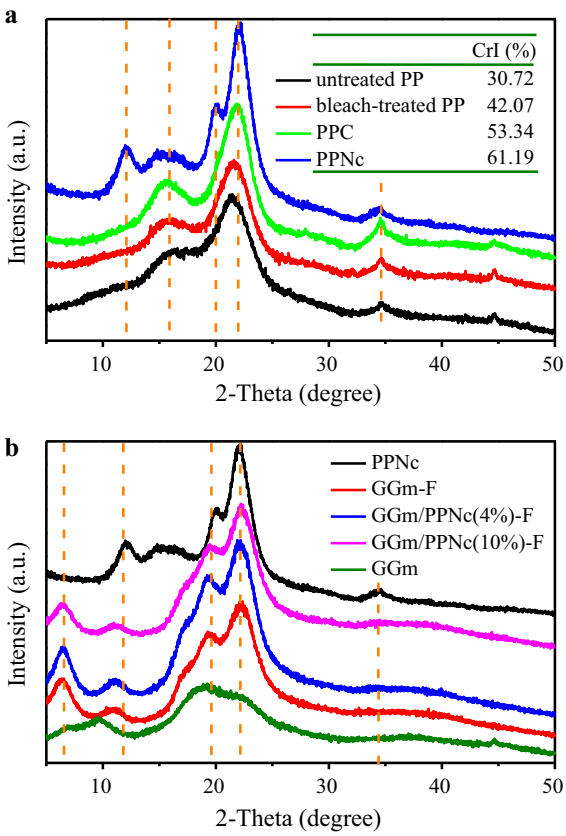

Fig. 2 XRD patterns of the untreated PP, bleach-treated PP, PPC and PPNc (**a**), and GGm, GGm-F, GGm/PPNc(4%)-F and GGm/PPNc(10%)-F (**b**)

were 30.72, 42.07, 53.34 and 61.19% respectively. Compared with the untreated PP, the increased CrI values for the bleach-treated PP and PPC could be ascribed to the efficient removals of lignin and hemicellulose by bleaching and alkali treatments, respectively. The subsequent increase of the CrI value for PPNc was further attributed to the dissolution of amorphous cellulosic domains in PPC. During the process of acid hydrolysis, hydronium ions (H_3O^+) could easily penetrate into the amorphous regions of the cellulose and induce partial hydrolytic cleavage of the glycosidic bonds inside the cellulose chains, consequently resulting in the release of the individual crystallite segments (Chen et al. 2016). Similar behaviors also were reported for the preparation of nanocelluloses from other bio-resources (Feng et al. 2015; Flauzino Neto et al. 2013; Johar et al. 2012; Santos et al. 2013). Consequently, significant increase of cellulose crystallinity could improve the stiffness and strength of cellulose due to the more ordered and compact molecular assemblies (Johar et al. 2012; Li et al. 2014). Hence, PPNc isolated from pineapple peel shows its potential in improving mechanical properties of composite materials.

The XRD patterns of the prepared films (GGm-F, GGm/PPNc(4%)-F and GGm/PPNc(10%)-F) are shown in Fig. 2b and compared with their initial substrates (GGm and PPNc respectively). For GGm, two broad peaks with low intensity were observed at $2\theta = 9.1°$ and 19.7° as similarly reported by Yang et al. (2013). Compared with PPNc and GGm, a new peak at $2\theta = 6.4°$ appeared in the XRD patterns of the prepared films. It was clearly seen that the introduction of PPNc in the films increased the crystallinity of the films. This phenomenon can be ascribed to the anchoring effect of the cellulosic filler acting as nucleating agents for the crystallization of polymer (Chaichi et al. 2017).

Morphological analysis

In order to investigate the structural changes of pineapple peel fibre before and after treatments, SEM images of the untreated-PP, bleach-treated PP, PPC and PPNc are shown in Fig. 3. It can be observed significantly that the morphological structures of the untreated and treated PP samples were quite different from each other. The untreated PP showed an irregular surface due to the existence of cementing materials around the cellulose fibres including pectin, hemicellulose and lignin (Li et al. 2014). After bleaching treatment, the obtained bleach-treated PP revealed a rougher but more ordered surface, due to the removal of the outer non-cellulosic layer composed mainly of lignin. Subsequently, after the alkali treatment, the obtained PPC exhibited more ordered and uniform fibril surface due to the removals of the hemicellulose and other noncellulosic components (Nepomuceno et al. 2017). Furthermore, a decrease from 30 to 10 μm in diameter was observed as PP was converted into PPC, indicating the partial separation of fibre bundles and the formation of individual fibre. For PPNc, the AFM image presented a needle-like structure throughout with averages of 15 ± 5 and 189 ± 23 nm in diameter and length respectively calculated by the ImageJ software, confirming the successful isolation of nanocellulose from pineapple peel. Although the liquid nanocellulose was cast onto a freshly cleaned

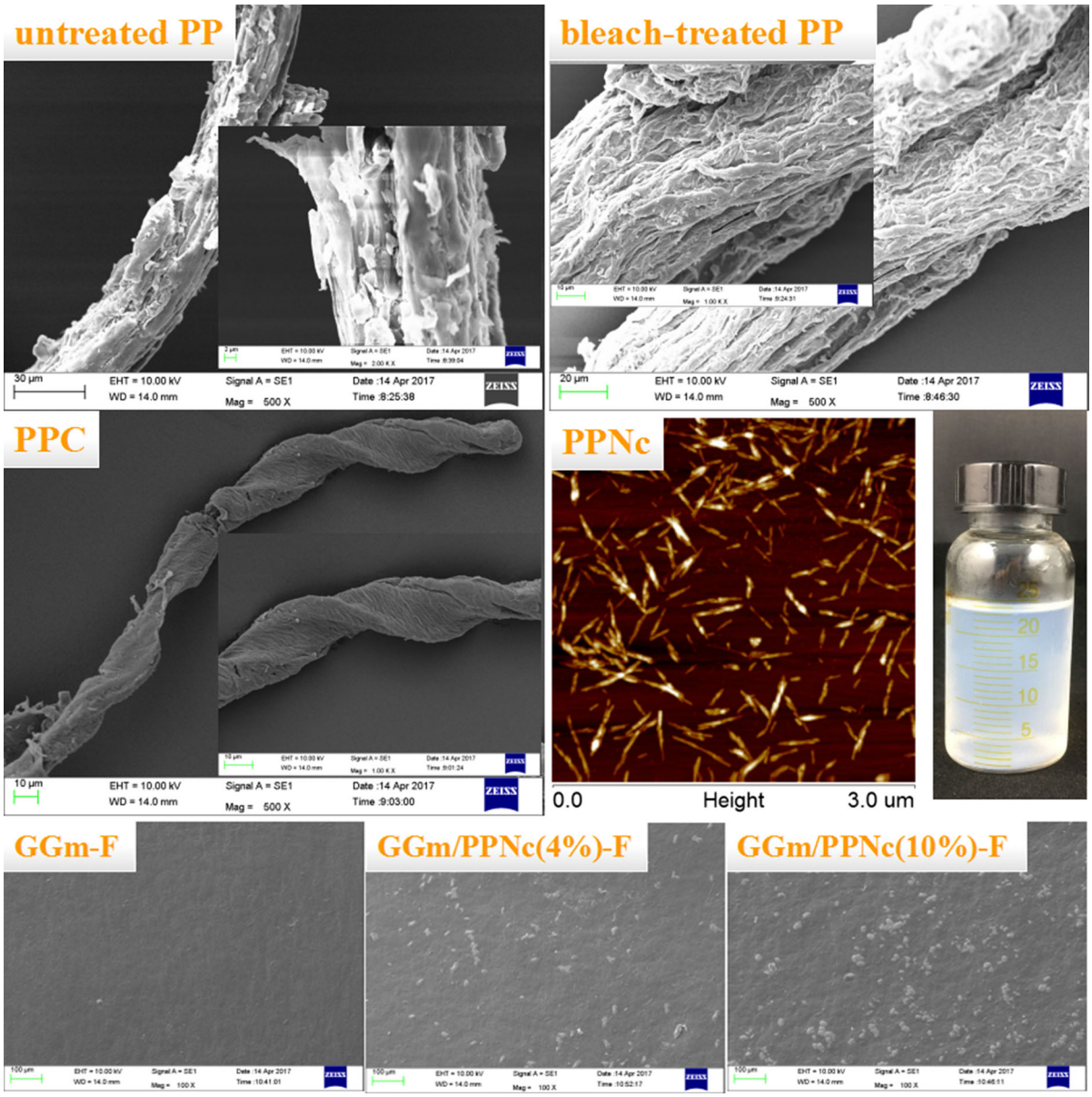

Fig. 3 AFM image of PPNc and SEM images of the untreated PP, bleach-treated PP, PPC, GGm-F, GGm/PPNc(4%)-F and GGm/PPNc(10%)-F

hydrophilic mica surface at a very low concentration (0.01wt%), there was a tendency to form agglomeration sites. The AFM image of nanocellulose isolated from other natural sources also proved this phenomenon (Nepomuceno et al. 2017; Santos et al. 2013). After storage at 4 °C for 5 months, the PPNc suspension was still stable without obvious precipitation, which could be ascribed to the imparted electrostatic stability for PPNc from the SO_4^{2-} groups (Feng et al. 2015). The PPNc suspension was detected to have a negative zeta potential of − 36.7 ± 0.2 mV. Generally, a stable suspension must have a zeta potential value lower than − 25.0 mV suspension (Ditzel et al. 2017). Additionally, as shown in Scheme 1, the untreated PP was changed from brownish-orange into white in colour after bleaching and alkali treatments, due to the removal of non-cellulosic materials such as lignin, hemicelluloses,

pectin and wax (Johar et al. 2012). After freeze-drying, the dried PPNc appeared a fluffy rime-like state. This observed white colour of PPC and PPNc was a clear indication of almost pure cellulosic materials, which was also confirmed by FITR and SEM results.

As shown in the SEM images of the prepared films, GGm-F exhibited a flat and smooth surface without impurity distribution. However, after addition of PPNc, the surface of GGm/PPNc-F showed many white dispersed particles as the increase of PPNc, which was probably due to the agglomeration or inhomogeneous dispersion of PPNc in the films. This phenomenon can be observed much more clearly in GGm/PPNc(10%)-F due to its higher PPNc concentration. Similar observation was also reported for bionanocomposite films prepared with agar and paper-mulberry pulp nanocellulose (Reddy and Rhim 2014).

Thermal stability analysis

The TG and DTG curves of pineapple peel fibre (including the untreated PP, bleach-treated PP, PPC and PPNc), GGm and the prepared films (including GGm-F, GGm/PPNc(4%)-F and GGm/PPNc(10%)-F) are shown in Fig. 4. As can be seen from this figure, an initial weight loss below 150 °C appeared in all samples due to the evaporation of water or low molecular weight compounds of these samples (Dai and Huang 2017a, b; Santos et al. 2013). The untreated PP started to degrade at around 217 °C and showed two dominant peaks of degradation at 287 and 347 °C on the DTG curve, while the bleach-treated PP and PPC began to degrade at 240 and 245 °C respectively and exhibited two peaks for bleach-treated PP at 292 and 349 °C and one peak for PPC at 351 °C on their DTG curves. Compared with the untreated PP, the higher initial degradation temperature for the bleach-treated PP and PPC could be attributed to the removal of hemicellulose, lignin and pectin which were known to have lower thermal stability than cellulose (Li et al. 2014). However, the PPNc exhibited significantly different degradation behavior compared with other samples, for which, the lower initial degradation temperature and broader degradation range of temperature were observed. This could be attributed to the drastic reduction in molecular weight and degradation of highly sulfated amorphous regions inside PPNc after acid hydrolysis (Mandal and Chakrabarty 2011). As depicted in the DTG curve of PPNc, the lower temperature stage (150–250 °C) with a peak at 190 °C was ascribed to the degradation of sulfated amorphous regions, while the higher temperature stage (300–400 °C) with a peak at 370 °C was due to the decomposition of the unsulfated crystal interior (Mandal and Chakrabarty 2011; Teixeira et al. 2011). After being heated to 500 °C, the untreated PP remained 24.01% of its initial mass, higher than the bleach-treated PP (22.34%) and PPC (18.41%). The lower residues can be attributed to the efficient removal of hemicellulose, lignin and silica ash during the sequential treatments (Johar et al. 2012; Li et al. 2014). However, it was worth noting that the PPNc showed the most remnant (32.09%), probably owing to the sulfated amorphous and crystalline regions of PPNc which act as a flame retardant during the degradation process (Johar et al. 2012; Roman and Winter 2004).

The thermal stability of the materials is essential in determining their processing temperature for application. Figure 4 clearly exhibits the enhancement in thermal stability of GGm/PPNc films as compared to GGm film. By addition of PPNc, the initial degradation at 161 °C for GGm-F was increased to 165 °C for GGm/PPNc(4%)-F and 171 °C for GGm/PPNc(10%)-F, implying the positive effect of PPNc on thermal stability of the films. As observed for the DTG curves, addition of PPNc also resulted in a slight increase of degradation rate, reaching higher maximum degradation rate of 243 °C for GGm/PPNc(4%)-F and 244 °C for GGm/PPNc(10%)-F, slightly higher than 241 °C for GGm-F. After being heated to 500 °C, GGm/PPNc(10%)-F remained the most residues (30.28%), higher than GGm/PPNc(4%)-F (21.47%) and GGm-F (20.38%). This phenomenon could be largely explained by the presence of higher amount of crystalline cellulose I from PPNc which had an intrinsically flame resistant characteristic (Haafiz et al. 2013).

Rheological studies

Figure 5a presents the shear viscosity of the aqueous solutions containing 1% of gellan gum and varied amount of PPNc (respectively 0, 2, 4, 6, 8 and 10% of gellan gum, w/w) as a function of shear rate. As can be seen from Fig. 5a, the shear viscosity of all the aqueous solutions could be divided into two distinct regions, including shear thinning (Pseudo plastic) and Newtonian regions (Chirayil et al. 2014). The

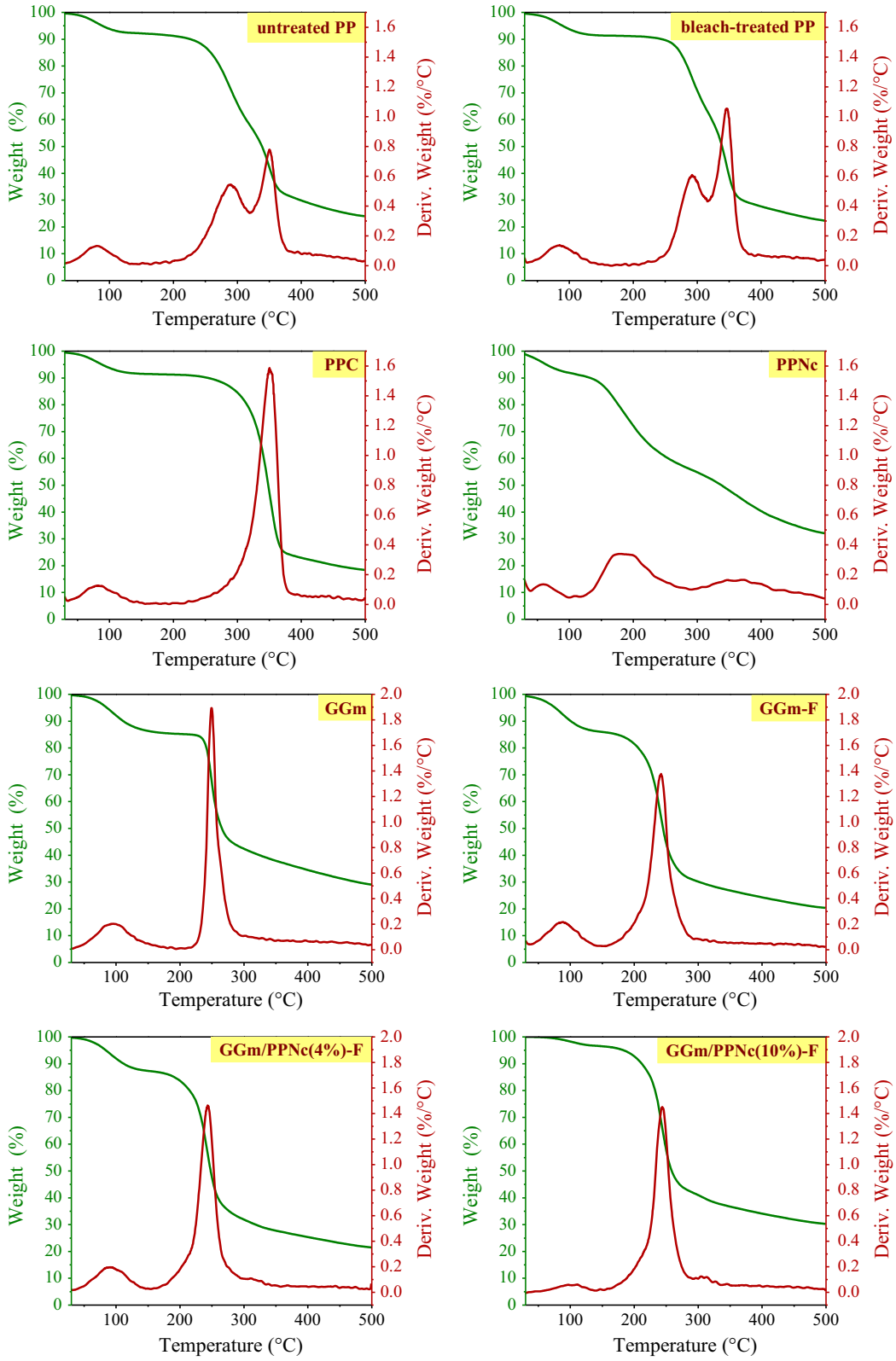
untreated PP
bleach-treated PP
PPC
PPNc
GGm
GGm-F
GGm/PPNc(4%)-F
GGm/PPNc(10%)-F
Weight (%)
Deriv. Weight (%/°C)
Temperature (°C)

◀**Fig. 4** TG and DTG curves of pineapple peel fibres (the untreated PP, bleach-treated PP, PPC and PPNc), GGm and the prepared films (GGm-F, GGm/PPNc(4%)-F and GGm/PPNc(10%)-F)

prepared aqueous solutions showed obvious shear thinning behaviour, in which the viscosity decreased significantly with increase of shear rate at the low shear region. This behaviour could be attributed to the formation and then break-up of hydrogen bonds in the aqueous solutions (Wu et al. 2017). The GGm/PPNc solutions exhibited increased shear viscosity with the increase of PPNc concentration, probably due to the abundant hydroxyl groups on the surface of PPNc which could induce formation of more hydrogen bonds (Wu et al. 2017). Subsequently, the solutions showed Newtonian behaviour as the shear rate was increased to 60 s^{-1}, henceforth viscosity was independent of shear rate.

Light transmittance of the films

The light transmittance (Tr) values of the prepared films within the wavelength range of 200–900 nm are shown in Fig. 5b. Compared with GGm-F, GGm/PPNc-F exhibited decreased Tr values with the increase of PPNc concentration, indicating that addition of PPNc in GGm decreased the transparency of the films. For example, at a wavelength of 800 nm, the Tr values of GGm/PPNc(2%)-F and GGm/F were 66.99 and 69.66%, respectively. However, in the case of GGm/PPNc(10%)-F, the Tr value decreased to 62.95%, obviously lower than the transparency of GGm/F. The high content of nanocellulose in the films

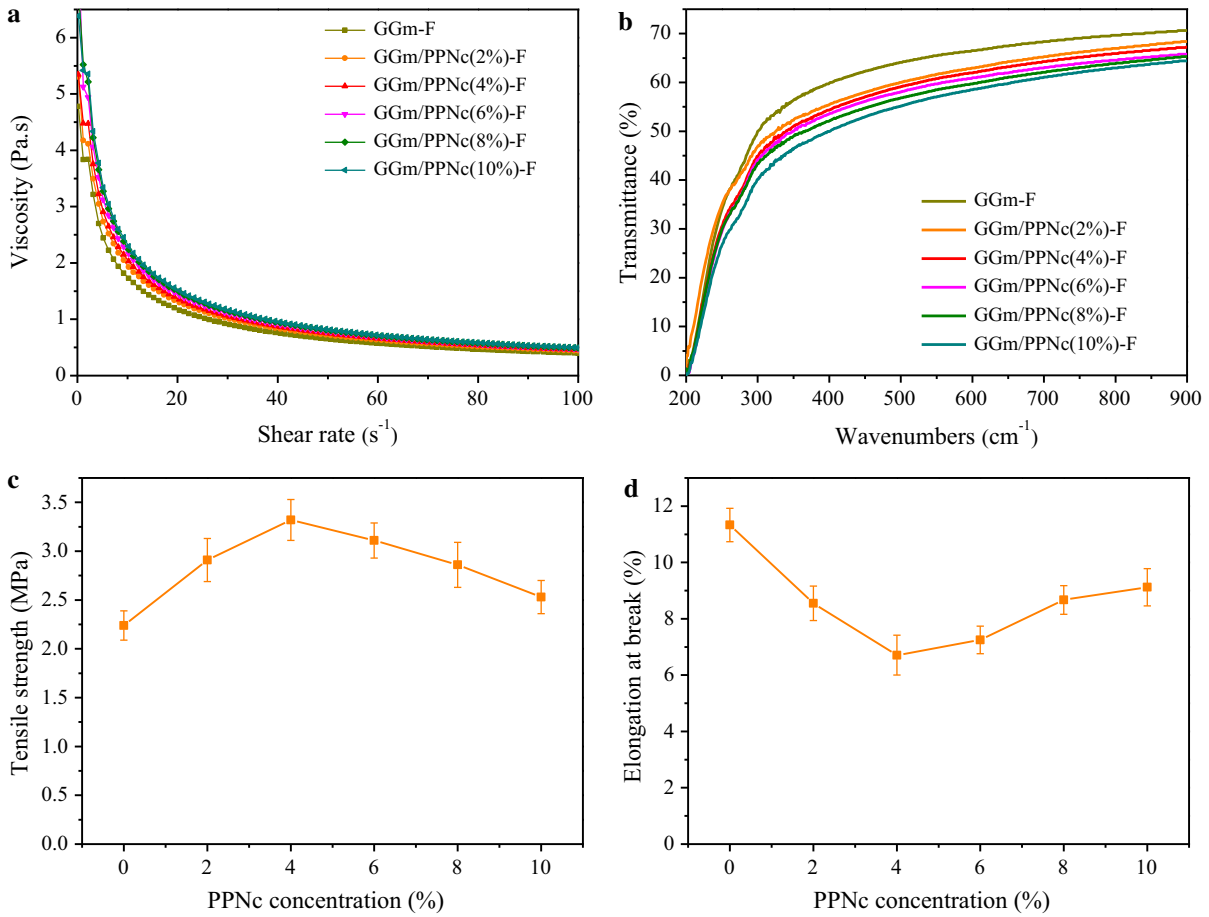

Fig. 5 Rheological analysis on GGm/PPNc aqueous solutions for films preparation (**a**), light transmittance of the prepared films (**b**), and the mechanical properties of the films, including tensile strength (**c**) and percentage elongation (**d**)

may contribute to the particle aggregate phenomenon, consequently resulting in the scattering and the decrease of transparency (Ma et al. 2011).

Mechanical properties

The mechanical properties such as tensile strength (TS) and percentage elongation at break (%E) of the prepared films are depicted in Fig. 5c, d. The TS and %E values of the neat GGm film (0% addition of PPNc) were 2.24 MPa and 11.33%, respectively. It was observed that the addition of PPNc enhanced the mechanical properties of the films. As shown in Fig. 5c, TS of GGm/PPNc films was firstly increased with the increase of PPNc concentration until up to 4%, and then started to decrease as further increase of the concentration. Compared with the neat GGm film, GGm/PPNc film (4% addition of PPNc) was improved by 48.21% of TS, which could be attributed to the geometry and rigidity of the PPNc and the formation of intermolecular forces between PPNc and GGm linked by hydrogen bonding (Chaichi et al. 2017). However, 6, 8 and 10% addition of PPNc only showed improvement by 38.84, 27.68 and 12.95%, respectively. The relatively decreased TS values of the GGm/PPNc films may be ascribed to the aggregation of PPNc inside GGm matrix due to Van der Waal's forces (Haafiz et al. 2013). Savadekar and Mhaske (2012) also reported that excess of nanocellulose content inside films would lead to a decreased TS due to phase separation, poor particle distribution and larger agglomerates formation. Generally, %E values of the films (as shown in Fig. 5d) were varied inversely with TS, which was consistent with current research results. A similar phenomenon was also observed in the starch-based film and kappa-carrageenan-based film reinforced by nanocellulose (Savadekar et al. 2012; Savadekar and Mhaske 2012).

Conclusion

The needle-like nanocellulose (PPNc), isolated from pineapple peel using sulfuric acid hydrolysis preceded by bleaching and alkali treatments, was used to reinforce gellan gum film. SEM, FTIR and XRD results confirmed the removal of non-cellulosic components for PPNc preparation. The PPNc presented high crystallinity about 61.19% and averages of 15 ± 5 and 189 ± 23 nm in diameter and length respectively. After being heated to 500 °C, PPNc showed the most remnant (32.09%), obviously higher than the untreated PP (24.01%), bleach-treated PP (22.34%) and PPC (18.41%). For film application, after being mixed with gellan gum solution, PPNc/gellan gum dispersions increased slightly in viscosities with the increase of nanocellulose content. PPNc was proved to be an excellent reinforcement for the gellan gum film via the increased crystallinity, thermal stability and tensile strength.

Acknowledgments This work was supported by the National Natural Science Foundation of China under Grant Nos. 31471673 and 31271978.

References

Abdul Khalil HPS, Davoudpour Y, Islam MN, Mustapha A, Sudesh K, Dungani R, Jawaid M (2014) Production and modification of nanofibrillated cellulose using various mechanical processes: a review. Carbohyd Polym 99: 649–655. https://doi.org/10.1016/j.carbpol.2013.08.069

Bhatnagar A, Sillanp M (2010) Utilization of agro-industrial and municipal waste materials as potential adsorbents for water treatment-A review. Chem Eng J 157:277–296. https://doi.org/10.1016/j.cej.2010.01.007

Brinchi L, Cotana F, Fortunati E, Kenny JM (2013) Production of nanocrystalline cellulose from lignocellulosic biomass: technology and applications. Carbohyd Polym 94:154–169. https://doi.org/10.1016/j.carbpol.2013.01.033

Chaichi M, Hashemi M, Badii F, Mohammadi A (2017) Preparation and characterization of a novel bionanocomposite edible film based on pectin and crystalline nanocellulose. Carbohyd Polym 157:167–175. https://doi.org/10.1016/j.carbpol.2016.09.062

Chang S, Kuo S, Wu C, Lee M, Niu CG, Liu W (2010) Gellan gum films for effective guided bone regeneration. J Med Biol Eng 30:99–103

Chen YW, Lee HV, Juan JC, Phang S (2016) Production of new cellulose nanomaterial from red algae marine biomass *Gelidium elegans*. Carbohyd Polym 151:1210–1219. https://doi.org/10.1016/j.carbpol.2016.06.083

Chirayil CJ, Mathew L, Hassan PA, Mozetic M, Thomas S (2014) Rheological behaviour of nanocellulose reinforced unsaturated polyester nanocomposites. Int J Biol Macromol 69: 274–281. https://doi.org/10.1016/j.ijbiomac.2014.05.055

Choonut A, Saejong M, Sangkharak K (2014) The production of ethanol and hydrogen from pineapple peel by *Saccharomyces cerevisiae* and *Enterobacter aerogenes*. Energy Procedia 52:242–249. https://doi.org/10.1016/j.egypro.2014.07.075

Criado P, Fraschini C, Salmieri S, Becher D, Safrany A, Lacroix M (2015) Evaluation of antioxidant cellulose nanocrystals and applications in gellan gum films. Ind Biotech 11:59–68. https://doi.org/10.1089/ind.2014.0017

Dai H, Huang H (2016) Modified pineapple peel cellulose hydrogels embedded with sepia ink for effective removal of methylene blue. Carbohyd Polym 148:1–10. https://doi.org/10.1016/j.carbpol.2016.04.040

Dai H, Huang H (2017a) Synthesis, characterization and properties of pineapple peel cellulose-g-acrylic acid hydrogel loaded with kaolin and sepia ink. Cellulose 24:69–84. https://doi.org/10.1007/s10570-016-1101-0

Dai H, Huang H (2017b) Enhanced swelling and responsive properties of pineapple peel carboxymethyl cellulose-g-poly(acrylic acid-co-acrylamide) superabsorbent hydrogel by the introduction of carclazyte. J Agr Food Chem 65:565–574. https://doi.org/10.1021/acs.jafc.6b04899

Dai H, Ou S, Liu Z, Huang H (2017) Pineapple peel carboxymethyl cellulose/polyvinyl alcohol/mesoporous silica SBA-15 hydrogel composites for papain immobilization. Carbohyd Polym 169:504–514. https://doi.org/10.1016/j.carbpol.2017.04.057

Dai H, Ou S, Huang Y, Liu Z, Huang H (2018a) Enhanced swelling and multiple-responsive properties of gelatin/sodium alginate hydrogels by the addition of carboxymethyl cellulose isolated from pineapple peel. Cellulose 25:293–606. https://doi.org/10.1007/s10570-017-1557-6

Dai H, Huang Y, Huang H (2018b) Eco-friendly polyvinyl alcohol/carboxymethyl cellulose hydrogels reinforced with graphene oxide and bentonite for enhanced adsorption of methylene blue. Carbohyd Polym 185:1–11. https://doi.org/10.1016/j.carbpol.2017.12.073

Ditzel FI, Prestes E, Carvalho BM, Demiate IM, Pinheiro LA (2017) Nanocrystalline cellulose extracted from pine wood and corncob. Carbohyd Polym 157:1577–1585. https://doi.org/10.1016/j.carbpol.2016.11.036

Dufresne A (2013) Nanocellulose: a new ageless bionanomaterial. Mater Today 16:220–227. https://doi.org/10.1016/j.mattod.2013.06.004

Feng X, Meng X, Zhao J, Miao M, Shi L, Zhang S, Fang J (2015) Extraction and preparation of cellulose nanocrystals from dealginate kelp residue: structures and morphological characterization. Cellulose 22:1763–1772. https://doi.org/10.1007/s10570-015-0617-z

Flauzino Neto WP, Silvério HA, Dantas NO, Pasquini D (2013) Extraction and characterization of cellulose nanocrystals from agro-industrial residue-Soy hulls. Ind Crop Prod 42:480–488. https://doi.org/10.1016/j.indcrop.2012.06.041

Foo KY, Hameed BH (2012) Porous structure and adsorptive properties of pineapple peel based activated carbons prepared via microwave assisted KOH and K_2CO_3 activation. Micropor Mesopor Mat 148:191–195. https://doi.org/10.1016/j.micromeso.2011.08.005

French AD (2014) Idealized powder diffraction patterns for cellulose polymorphs. Cellulose 21:885–896. https://doi.org/10.1007/s10570-013-0030-4

Haafiz MKM, Hassan A, Zakaria Z, Inuwa IM, Islam MS, Jawaid M (2013) Properties of polylactic acid composites reinforced with oil palm biomass microcrystalline cellulose. Carbohyd Polym 98:139–145. https://doi.org/10.1016/j.carbpol.2013.05.069

Haafiz MKM, Hassan A, Zakaria Z, Inuwa IM (2014) Isolation and characterization of cellulose nanowhiskers from oil palm biomass microcrystalline cellulose. Carbohyd Polym 103:119–125. https://doi.org/10.1016/j.carbpol.2013.11.055

Hu K, Hu X, Zeng L, Zhao M, Huang H (2010) Hydrogels prepared from pineapple peel cellulose using ionic liquid and their characterization and primary sodium salicylate release study. Carbohyd Polym 82:62–68. https://doi.org/10.1016/j.carbpol.2010.04.023

Hu L, Zheng G, Yao J, Liu N, Weil B, Eskilsson M, Karabulut E, Ruan Z, Fan S, Bloking JT, McGehee MD (2013a) Transparent and conductive paper from nanocellulose fibers. Energy Environ Sci 6:513–518. https://doi.org/10.1039/C2EE23635D

Hu X, Wang J, Huang H (2013b) Impacts of some macromolecules on the characteristics of hydrogels prepared from pineapple peel cellulose using ionic liquid. Cellulose 20:2923–2933. https://doi.org/10.1007/s10570-013-0075-4

Ismail NA, Mohamad SF, Ibrahim MA, Amin KAM (2014) Evaluation of gellan gum film containing virgin coconut oil for transparent dressing materials. Adv Biomater 2014:1–12

Johar N, Ahmad I, Dufresne A (2012) Extraction, preparation and characterization of cellulose fibres and nanocrystals from rice husk. Ind Crop Prod 37:93–99. https://doi.org/10.1016/j.indcrop.2011.12.016

Karim AA, Bhat R (2008) Gelatin alternatives for the food industry: recent developments, challenges and prospects. Trends Food Sci Technol 19:644–656. https://doi.org/10.1016/j.tifs.2008.08.001

Kaur N, Sharma S, Kaur S, Khosla E (2016) Reverse micellar extraction of acid dyes from simulated textile effluent. J Chem Biol Phys Sci (JCPBS) 6:180–197

Khawas P, Deka SC (2016) Isolation and characterization of cellulose nanofibers from culinary banana peel using high-intensity ultrasonication combined with chemical treatment. Carbohyd Polym 137:608–616. https://doi.org/10.1016/j.carbpol.2015.11.020

Krishni RR, Hameed KYFB (2014) Food cannery effluent, pineapple peel as an effective low-cost biosorbent for removing cationic dye from aqueous solutions. Desalin Water Treatm 52:6096–6103. https://doi.org/10.1080/19443994.2013.815686

Kulkarni RV, Mangond BS, Mutalik S, Sa B (2011) Interpenetrating polymer network microcapsules of gellan gum and egg albumin entrapped with diltiazem–resin complex for controlled release application. Carbohyd Polym 83:1001–1007. https://doi.org/10.1016/j.carbpol.2010.09.017

Lagerwall JPF, Schütz C, Salajkova M, Noh J, Hyun Park J, Scalia G, Bergstr ML (2014) Cellulose nanocrystal-based materials: from liquid crystal self-assembly and glass formation to multifunctional thin films. NPG Asia Mater 6:e80. https://doi.org/10.1038/am.2013.69

Lee M, Tsai H, Wen S, Huang C (2012) Photocrosslinkable gellan gum film as an anti-adhesion barrier. Carbohyd Polym 90:1132–1138. https://doi.org/10.1016/j.carbpol.2012.06.064

Li M, Wang L, Li D, Cheng Y, Adhikari B (2014) Preparation and characterization of cellulose nanofibers from depectinated sugar beet pulp. Carbohyd Polym 102:136–143. https://doi.org/10.1016/j.carbpol.2013.11.021

Ma H, Zhou B, Li Y, Li H, Ou S (2011) Green composite films composed of nanocrystalline cellulose and a cellulose matrix regenerated from functionalized ionic liquid

solution. Carbohyd Polym 84:383–389. https://doi.org/10.1016/j.carbpol.2010.11.050

Mandal A, Chakrabarty D (2011) Isolation of nanocellulose from waste sugarcane bagasse (SCB) and its characterization. Carbohyd Polym 86:1291–1299. https://doi.org/10.1016/j.carbpol.2011.06.030

Morais JOPS, Rosa MDF, de Souza FM, Nascimento LD, Do Nascimento DME, Cassales AR (2013) Extraction and characterization of nanocellulose structures from raw cotton linter. Carbohyd Polym 91:229–235. https://doi.org/10.1016/j.carbpol.2012.08.010

Nam S, French AD, Condon BD, Concha M (2016) Segal crystallinity index revisited by the simulation of X-ray diffraction patterns of cotton cellulose Iβ and cellulose II. Carbohyd Polym 135:1–9. https://doi.org/10.1016/j.carbpol.2015.08.035

Nepomuceno NC, Santos ASF, Oliveira JE, Glenn GM, Medeiros ES (2017) Extraction and characterization of cellulose nanowhiskers from *Mandacaru* (*Cereus jamacaru* DC.) spines. Cellulose 24:119–129. https://doi.org/10.1007/s10570-016-1109-5

Reddy JP, Rhim J (2014) Characterization of bionanocomposite films prepared with agar and paper-mulberry pulp nanocellulose. Carbohyd Polym 110:480–488. https://doi.org/10.1016/j.carbpol.2014.04.056

Roman M, Winter WT (2004) Effect of sulfate groups from sulfuric acid hydrolysis on the thermal degradation behavior of bacterial cellulose. Biomacromolecules 5:1671–1677. https://doi.org/10.1021/bm034519+

Saelo S, Assatarakul K, Sane A, Suppakul P (2016) Fabrication of novel bioactive cellulose-based films derived from caffeic acid phenethyl ester-loaded nanoparticles via a rapid expansion process: RESOLV. J Agric Food Chem 64:6694–6707. https://doi.org/10.1021/acs.jafc.6b02197

Santos RMD, Flauzino Neto WP, Silvério HA, Martins DF, Dantas NO, Pasquini D (2013) Cellulose nanocrystals from pineapple leaf, a new approach for the reuse of this agro-waste. Ind Crop Prod 50:707–714. https://doi.org/10.1016/j.indcrop.2013.08.049

Savadekar NR, Mhaske ST (2012) Synthesis of nano cellulose fibers and effect on thermoplastics starch based films. Carbohyd Polym 89:146–151. https://doi.org/10.1016/j.carbpol.2012.02.063

Savadekar NR, Karande VS, Vigneshwaran N, Bharimalla AK, Mhaske ST (2012) Preparation of nano cellulose fibers and its application in kappa-carrageenan based film. Int J Biol Macromol 51:1008–1013. https://doi.org/10.1016/j.ijbiomac.2012.08.014

Shankar S, Rhim J (2016) Preparation of nanocellulose from micro-crystalline cellulose: the effect on the performance and properties of agar-based composite films. Carbohyd Polym 135:18–26. https://doi.org/10.1016/j.carbpol.2015.08.082

Sharmin N, Khan RA, Salmieri S, Dussault D, Bouchard J, Lacroix M (2012) Modification and characterization of biodegradable methylcellulose films with trimethylolpropane trimethacrylate (TMPTMA) by γ radiation: effect of nanocrystalline cellulose. J Agric Food Chem 60:623–629. https://doi.org/10.1021/jf203500s

Teixeira EDM, Bondancia TJ, Teodoro KBR, Corrêa AC, Marconcini JM, Mattoso LHC (2011) Sugarcane bagasse whiskers: extraction and characterizations. Ind Crop Prod 33:63–66. https://doi.org/10.1016/j.indcrop.2010.08.009

Trache D, Hussin MH, Haafiz MKM, Thakur VK (2017) Recent progress in cellulose nanocrystals: sources and production. Nanoscale 9:1763–1786. https://doi.org/10.1039/C6NR09494E

Wu G, Liu G, Chen J, Kong Z (2017) Preparation and properties of thermoset composite films from two-component waterborne polyurethane with low loading level nanofibrillated cellulose. Prog Org Coat 106:170–176. https://doi.org/10.1016/j.porgcoat.2016.10.031

Xu X, Li B, Kennedy JF, Xie BJ, Huang M (2007) Characterization of konjac glucomannan–gellan gum blend films and their suitability for release of nisin incorporated therein. Carbohyd Polym 70:192–197. https://doi.org/10.1016/j.carbpol.2007.03.017

Yang F, Xia S, Tan C, Zhang X (2013) Preparation and evaluation of chitosan–calcium–gellan gum beads for controlled release of protein. Eur Food Res Technol 237:467–479. https://doi.org/10.1007/s00217-013-2021-y

Zhang YD, Xia XZ (2012) Physicochemical Characteristics of pineapple (*Ananas mill.*) peel cellulose prepared by different methods. Adv Mater Res 554:1038–1041. https://doi.org/10.4028/www.scientific.net/AMR.554-556.1038

Zhang H, Yang M, Luan Q, Tang H, Huang F, Xiang X, Yang C, Bao Y (2017a) Cellulose anionic hydrogels based on cellulose nanofibers as natural stimulants for seed germination and seedling growth. J Agr Food Chem 65:3785–3791. https://doi.org/10.1021/acs.jafc.6b05815

Zhang N, Xu J, Gao X, Fu X, Zheng D (2017b) Factors affecting water resistance of alginate/gellan blend films on paper cups for hot drinks. Carbohyd Polym 156:435–442. https://doi.org/10.1016/j.carbpol.2016.08.101